A&A 484, 17–28 (2008)
DOI: 10.1051/0004-6361:20078819

Astronomy & Astrophysics

Three-fluid plasmas in star formation

II. Momentum transfer rate coefficients

C. Pinto[1] and D. Galli[2]

[1] Dipartimento di Astronomia e Scienza dello Spazio, Università di Firenze, Largo E. Fermi 5, 50125 Firenze, Italy
e-mail: cecilia@arcetri.astro.it
[2] INAF – Osservatorio Astrofisico di Arcetri, Largo E. Fermi 5, 50125 Firenze, Italy

Received 9 October 2007 / Accepted 16 February 2008

ABSTRACT

Context. The charged component of the insterstellar medium consists of atomic and molecular ions, electrons, and charged dust grains, coupled to the local Galactic magnetic field. Collisions between neutral particles (mostly atomic or molecular hydrogen) and charged species, and between the charged species themselves, affect the magnetohydrodynamical behaviour of the medium and the dissipation of electric currents.
Aims. The friction force due to elastic collisions between particles of different species in the multi-component interstellar plasma is a nonlinear function of the temperature of each species and the Mach number of the relative drift velocity. The aim of this paper is to provide an accurate and, as far as possible, complete set of momentum transfer rate coefficients for magnetohydrodynamical studies of the interstellar medium.
Methods. Momentum transfer rates are derived from available experimental data and theoretical calculations of cross sections within the classic approach developed by Boltzmann and Langevin for a wide range of values of the temperature and the drift velocity.
Results. Accurate numerical values for momentum transfer rates are obtained and fitted to simple analytical formulae expressing the dependence of the results on the gas temperature and the relative drift velocity. The often used polarization approximation is in satisfactory agreement with our results only for collisions between H_2 and molecular ions (HCO^+, H_3^+). For other kinds of collisions, the polarization approximation fails by large factors, and must be replaced by more accurate expressions.

Key words. atomic processes – molecular processes – plasmas – magnetohydrodynamics (MHD) – ISM: clouds – ISM: jets and outflows

1. Introduction

The interstellar medium (ISM) is a multi-component plasma that consists mostly of hydrogen, helium, heavy ions, electrons and charged dust grains. The interaction between these components, and their coupling with the Galactic magnetic field, determine the dynamical properties of the ISM, control its evolution and the nature of the star formation process. In particular, the momentum exchange in collisions between neutral and charged particles is responsible for transfering the effects of electric and magnetic forces to the neutral component, allowing the magnetic field to drift out of weakly-ionized molecular clouds (Mestel & Spitzer 1956), damping the propagation of Alfvèn waves (Zweibel & Josafatsson 1983), and heating the gas by the frictional dissipation of turbulent energy (Scalo 1977).

In a companion paper (Pinto et al. 2008, hereafter Paper I), we have derived the equations governing the dynamics of a three-fluid system, reducing the set of equations to a momentum equation for the mean fluid and an evolution equation for the magnetic field, plus two relations for the drift velocities in terms of the mean fluid velocity and the magnetic field.

In this paper, we report on a detailed analysis of collisional rate coefficients involving the most abundant neutral and charged species in the ISM. The paper is organized as follows: in Sect. 2, we give the general expression for the friction force and the momentum transfer rate coefficient for elastic collisions, and we obtain an analytical solution for a cross section varying as a power of the relative velocity; in Sect. 3, we consider collisions with H_2 of HCO^+, H_3^+, H^+, and electrons, using available theoretical and/or experimental determination of the collision cross section; similarly, in Sect. 4, we consider collisions with H of C^+, H^+, and electrons; in Sect. 5, we consider collisions of H^+ and electrons with He; in Sects. 6 and 7 we consider collisions between charged dust grains and neutral particles, and between charged particles, respectively; in Sect. 8, we give analytical approximations for our numerical results; finally, in Sect. 9, we summarize our conclusions.

2. Friction force and rate coefficients

The general expression of the momentum acquired per unit time and unit volume ("friction force") by a particle of species s with mass m_s and initial velocity $\boldsymbol{v}_s$ ("test particle") through collisions with particles of species s' with mass $m_{s'}$ and initial velocity $\boldsymbol{v}_{s'}$ ("field particles") was given by Boltzmann (1896),

$$\boldsymbol{F}_{ss'} = n_s n_{s'} \int \mathrm{d}\boldsymbol{v}_s f(\boldsymbol{v}_s) \int \mathrm{d}\boldsymbol{v}_{s'} f(\boldsymbol{v}_{s'}) v_{ss'} \times \int \mathrm{d}\Omega \frac{\mathrm{d}\sigma}{\mathrm{d}\Omega} m_s(\boldsymbol{w}_s - \boldsymbol{v}_s), \quad (1)$$

where $f(\boldsymbol{v}_s)$ and $f(\boldsymbol{v}_{s'})$ are the velocity distribution functions of the two species, $\boldsymbol{w}_s$ is the velocity of the test particle after the collision, $\mathrm{d}\sigma/d\Omega$ is the differential scattering cross section, and $v_{ss'}$ is the relative velocity of the particles (before the collision),

$$v_{ss'} \equiv |\boldsymbol{v}_s - \boldsymbol{v}_{s'}|. \quad (2)$$

For elastic collisions, the last term in Eq. (1), representing the momentum change of the test particle after the collision, can be written as

$$\int \mathrm{d}\Omega \frac{\mathrm{d}\sigma}{\mathrm{d}\Omega} m_s(\boldsymbol{w}_s - \boldsymbol{v}_s) = \mu_{ss'}\sigma_{\mathrm{mt}}(\boldsymbol{v}_{s'} - \boldsymbol{v}_s), \tag{3}$$

where $\mu_{ss'} = m_s m_{s'}/(m_s + m_{s'})$ is the reduced mass of the system,

$$\sigma_{\mathrm{mt}} = \int \frac{\mathrm{d}\sigma}{\mathrm{d}\Omega}(1 - \cos\Theta)\,\mathrm{d}\Omega \tag{4}$$

is the momentum transfer cross section, and Θ is *scattering angle* in the center-of-mass system. Equation (1) reduces then to the expression

$$\boldsymbol{F}_{ss'} = \mu_{ss'} n_s n_{s'} \int \mathrm{d}\boldsymbol{v}_s f(\boldsymbol{v}_s) \int \mathrm{d}\boldsymbol{v}_{s'} f(\boldsymbol{v}_{s'}) v_{ss'} \sigma_{\mathrm{mt}}(\mathbf{v}_{s'} - \boldsymbol{v}_s). \tag{5}$$

The six integrations of Eq. (5) require some care because of the presence of the relative velocity in the integrand. When the velocity distribution of both species is Maxwellian with temperatures T_s and $T_{s'}$, the integrations can be carried out explicitly, as shown first by Langevin (1905), and the result is

$$\boldsymbol{F}_{ss'} = \alpha_{ss'}(\boldsymbol{u}_{s'} - \boldsymbol{u}_s), \tag{6}$$

where $\boldsymbol{u}_s$ and $\boldsymbol{u}_{s'}$ are the mean (Maxwellian) velocities of each species and the friction coefficient $\alpha_{ss'}$ is defined as

$$\alpha_{ss'} \equiv \mu_{ss'} n_s n_{s'} \langle\sigma v\rangle_{ss'}. \tag{7}$$

In this expression, $\langle\sigma v\rangle_{ss'}$ is an average of the momentum transfer cross section over the relative velocity of the interacting particles,

$$\langle\sigma v\rangle_{ss'} = a_{ss'} \frac{\mathrm{e}^{-\xi^2}}{2\sqrt{\pi}\xi^3} \times \int_0^\infty x^2 \mathrm{e}^{-x^2}[(2\xi x - 1)\mathrm{e}^{2\xi x} + (2\xi x + 1)\mathrm{e}^{-2\xi x}]\sigma_{\mathrm{mt}}\,\mathrm{d}x, \tag{8}$$

where the nondimensional variables ξ and x are defined by

$$\xi \equiv \frac{v_{\mathrm{d}}}{a_{ss'}}, \qquad x \equiv \frac{v_{ss'}}{a_{ss'}}, \tag{9}$$

and

$$v_{\mathrm{d}} \equiv |\boldsymbol{u}_s - \boldsymbol{u}_{s'}| \tag{10}$$

is the drift velocity, and

$$a_{ss'} \equiv \left(\frac{2kT_{ss'}}{\mu_{ss'}}\right)^{1/2}, \tag{11}$$

is the most probable velocity in a gas of particles of mass $\mu_{ss'}$ and temperature

$$T_{ss'} \equiv \frac{m_s T_{s'} + m_{s'} T_s}{m_s + m_{s'}}\,. \tag{12}$$

The quantity $\langle\sigma v\rangle_{ss'}$ is called the *momentum transfer rate coefficient*. A related quantity is the *collision frequency* between a test particle s and the incident particles s'

$$\nu_{ss'} = n_{s'}\langle\sigma v\rangle_{ss'}. \tag{13}$$

The momentum transfer rate coefficient defined by Eq. (8) is a function of the temperature $T_{ss'}$ and the drift velocity $|\boldsymbol{u}_{s'} - \boldsymbol{u}_s|$, with the parameters x and ξ playing the roles of Mach number for the collision and the drift velocity, respectively. Owing to the dependence of $\langle\sigma v\rangle_{ss'}$ on ξ, the friction force Eq. (6) is in general a nonlinear function of the drift velocity.

For a cross section varying as a power-law of the relative velocity, $\sigma(v_{ss'}) = \sigma_0 x^{-n}$, the integral in Eq. (8) can be expressed in terms of the confluent hypergeometric function $M(a, b, c)$ (Abramowitz & Stegun 1965),

$$\langle\sigma v\rangle_n = \sigma_0 a_{ss'} G_n(\xi), \tag{14}$$

where

$$G_n(\xi) = \frac{4}{3\sqrt{\pi}}\Gamma\left(3 - \frac{n}{2}\right)\exp(-\xi^2) M\left(3 - \frac{n}{2}, \frac{5}{2}, \xi^2\right). \tag{15}$$

For vanishing drift velocities $G_n(\xi)$ reduces to a constant factor, $G_n(0) = 4\Gamma(3 - n/2)/(3\sqrt{\pi})$, whereas in the opposite limit of large drift velocities $G_n(\xi) \approx \xi^{1-n}$. The behaviour of the function $G_n(\xi)$ for n = 0,1,2,3 and 4 is shown in Fig. 1.

Three special cases of Eq. (14) are relevant for collisions between ISM particles:

(*a*) $n = 0$, with

$$G_0(\xi) = \frac{1}{\sqrt{\pi}}\left(1 + \frac{1}{2\xi^2}\right)\mathrm{e}^{-\xi^2} + \left(\xi + \frac{1}{\xi} - \frac{1}{4\xi^3}\right)\mathrm{erf}(\xi); \tag{16}$$

(Baines et al. 1965). A cross section $\sigma_0 = \pi(r_s + r_{s'})^2$, independent on the relative velocity describes the collisions between solid particles, represented as "hard spheres" of radii r_s and $r_{s'}$.

(*b*) $n = 1$, with $G_1(\xi) = 1$. A cross section varying as the inverse of the relative velocity arises for an induced dipole attraction, where the interaction potential is proportional to the inverse fourth power of the distance ("polarization potential"). Particles obeying this particular interaction law are called "Maxwell molecules" (Maxwell 1860a,b), and the corresponding collisional rate coefficient "Langevin rate" (see Appendix). In this polarization approximation, the momentum transfer rate is independent of both temperature and drift velocity.

(*c*) $n = 4$, corresponding to a (screened) Coulomb potential, with

$$G_4(\xi) = \frac{\mathrm{erf}(\xi)}{\xi^3} - \frac{2\mathrm{e}^{-\xi^2}}{\sqrt{\pi}\xi^2}\,. \tag{17}$$

This result was first derived by Chandrasekhar (1943) in the context of stellar dynamics and, independently, by Dreicer (1959) and Sivukhin (1966) for a fully-ionized gas[1]. In many astrophysical applications, the relative velocity of the interacting particles is of the order of the sound speed in the gas (if the temperatures of the two species are not too different), but the drift velocity $|\boldsymbol{u}_{s'} - \boldsymbol{u}_s|$ is usually much lower than the sound speed. In such circumstances it is appropriate to expand the integrand in Eq. (8) for small values of the quantity ξx, obtaining, to the lowest order in the expansion, a value of the momentum transfer rate coefficient independent of the drift velocity,

$$\langle\sigma v\rangle_{ss'} \approx \frac{4}{3}\left(\frac{8\,k\mathrm{T}_{ss'}}{\pi\mu_{ss'}}\right)^{1/2} \int_0^\infty x^5 \mathrm{e}^{-x^2}\sigma_{\mathrm{mt}}(x)\,\mathrm{d}x + O(\xi^2). \tag{18}$$

[1] Draine & Salpeter (1979) give the following accurate approximations for $n = 0$ and $n = 4$:

$$G_0(\xi) \approx \frac{8}{3\sqrt{\pi}}\left(1 + \frac{9\pi}{64}\xi^2\right)^{1/2}, \qquad G_4(\xi) \approx \left(\frac{3\sqrt{\pi}}{4} + \xi^3\right)^{-1}.$$

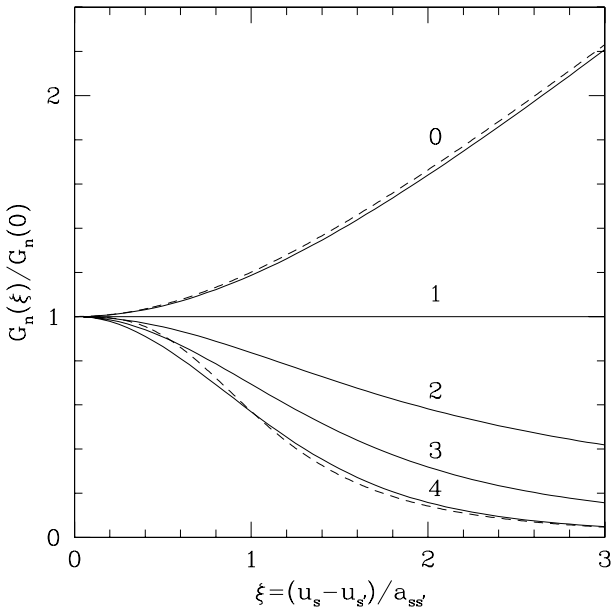

Fig. 1. The normalized function $G_n(\xi)/G_n(0)$ defined by Eq. (15) as function of the normalized drift velocity $\xi = |\boldsymbol{u}_s - \boldsymbol{u}_{s'}|/a_{ss'}$ with $n = 0$, 1, 2, 3, and 4 (*solid* curves). The *dashed* curves show the approximations given by Draine & Salpeter (1979) for the cases $n = 0$ and $n = 4$.

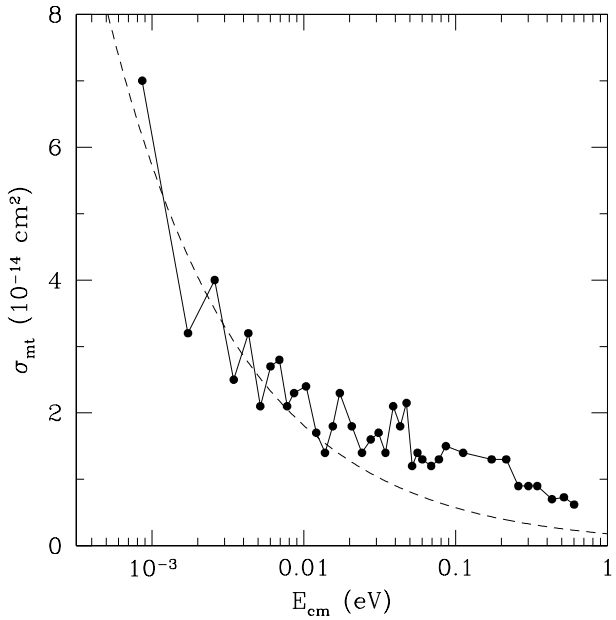

Fig. 2. The momentum transfer cross section for collisions HCO^+–H_2 as a function of E_{cm} computed by Flower (2000) (*dots* and *solid* curve). The *dashed* curve shows the Langevin cross section.

If the momentum transfer cross section is given in terms of the collision energy in the center-of-mass system $E_{cm} = \mu_{ss'} v_{ss'}^2/2$, the rate coefficient in the small drift limit can be written as

$$\langle\sigma v\rangle_{ss'} \approx \frac{2}{3}\left(\frac{8kT_{ss'}}{\pi\mu_{ss'}}\right)^{1/2} \int_0^\infty z^2 \mathrm{e}^{-z}\sigma_{mt}(z)\,\mathrm{d}z + O(\xi^2), \qquad (19)$$

where $z \equiv E_{cm}/kT_{ss'}$, a frequently-adopted expression (see e.g., Mitchner & Kruger 1973)[2].

3. Collisions with H_2

Collisions between H_2 molecules and charged particles determine the rate of diffusion of the interstellar magnetic field through the dominantly neutral gas of cold molecular clouds (see Paper I). In applications to molecular clouds (e.g., Nakano 1984; Mouschovias 1996), the collision rate coefficient $\langle\sigma v\rangle_{s,H_2}$ has usually been estimated with the polarization approximation (see Appendix) for collisions with molecular ions, and, also sometimes, for collisions with electrons (see discussion in Mouschovias 1996). For collisions between H_2 and dust grains, the hard sphere model (Sect. 2) has generally been assumed. We review below the validity of these assumptions and compute accurate values for the collision rate coefficients using available momentum transfer cross sections.

3.1. $HCO^+ - H_2$

Flower (2000) has calculated quantum-mechanically the cross section between HCO^+, a dominant ion in typical molecular cloud conditions, and H_2 molecules in their rotational ground states. Figure 2 shows the cross section computed by Flower (2000) compared with the Langevin cross section. As noticed by Flower (2000), the Langevin value gives a good approximation to the quantal results. The rate coefficient is, therefore, expected to depend very weakly on temperature and drift velocity, as shown in Fig. 3[3]. Previous estimates of the molecular ion-H_2 rate coefficient based on the Langevin formula (see Fig. 3) have ignored the weak dependence from temperature and drift velocity. This neglect is, however, of little consequence for models of magnetically-controlled cloud collapse as long as the temperature of the infalling gas is in the range 10–20 K and the ion-neutral drift velocity is a small fraction of the sound speed, as shown e.g., by Mouschovias & Ciolek (1994).

3.2. $H_3^+ - H_2$

Figure 4 shows the momentum transfer cross section for collisions of H_3^+ and H_2, recommended by Phelps (1990), converted to energies in the center-of-mass frame. At low energies ($E_{cm} \lesssim 1$ eV), the cross section is obtained from the results of the mobility experiments of Ellis et al. (1976). At higher energies, the behavior of the cross section is extrapolated from mobility data at room temperature. As shown in the figure, the cross section is very close to the Langevin value up to $E_{cm} \approx 3$ eV, but declines steeply (as $E_{cm}^{-1.7}$) above $E_{cm} \approx 10$ eV. Since the cross section tabulated by Phelphs (1990) does not extend to ion energies below 0.1 eV, we have extrapolated Phelps's value to lower energies with the asymptotic formula $\sigma_{mt} = 1.62 \times 10^{-15}(E_{cm}/\mathrm{eV})^{-0.507}$. Figure 5 shows the corresponding rate coefficient obtained integrating the cross section, according to Eq. (8) as a function of the temperature and for various values of the drift velocity. As in the case of HCO^+, given the Langevin behavior of the cross section at low energies, the dependence of the collisional rate from

[2] The momentum transfer cross section measured in laboratory experiments is usually given as function of the energy in the laboratory frame (E_{lab}). Before using Eq. (19), E_{lab} must be converted into the energy in the center-of-mass frame according to the formula

$$E_{cm} = \frac{m_s}{m_s + m_{s'}} E_{lab} + \frac{3m_{s'}}{2(m_s + m_{s'})} kT_s,$$

where s and s' indicate the target and incident particles, respectively.

[3] Our rate coefficient for zero drift velocity differs by ∼20% from the result by Flower (2000) who adopts an averaging over the particles kinetic energy slightly different from our Eq. (19).

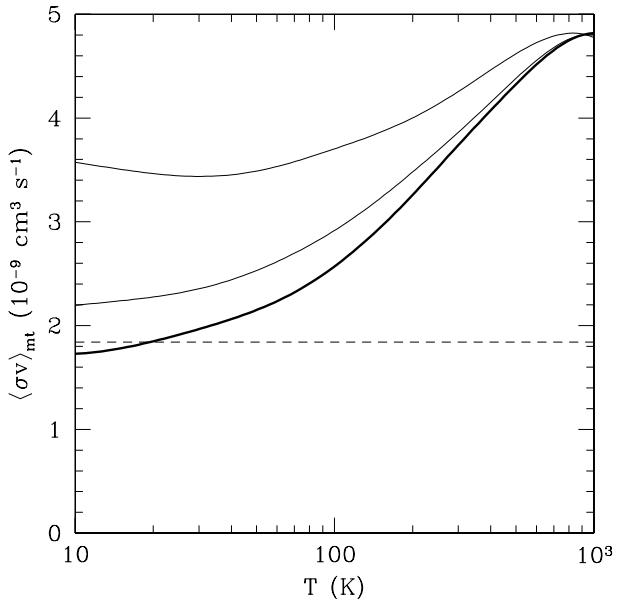

Fig. 3. The rate coefficient for HCO^+–H_2 collisions as a function of the temperature T for $v_d = 0$ (*thick solid* curve); and $v_d = 1$ km s^{-1}; $v_d = 2$ km s^{-1} (*thin solid* curves, bottom to top), compared with the Langevin rate (*dashed* line).

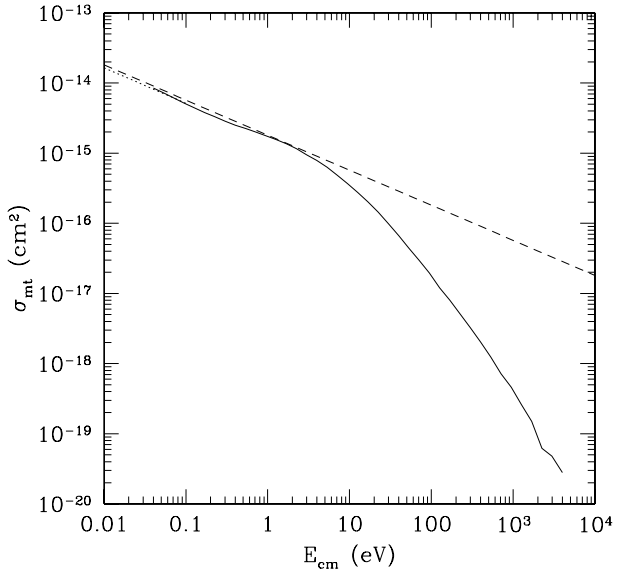

Fig. 4. Momentum transfer cross section for H_3^+–H_2 collisions as a function of the energy in the center-of-mass system according to Phelps (1990) (*solid* curve). The *dotted* line shows our extrapolation at low energies, whereas the *dashed* line shows the Langevin cross section.

temperature and drift velocity is very weak for temperatures below ~10^4 K.

3.3. $H^+ - H_2$

Figure 6 shows the momentum transfer cross section for H^+–H_2 collisions computed by Krstić & Schultz (1999a,c) in the energy range 0.1 eV < E_{cm} < 100 eV (fully-quantal calculation), by Bachmann & Reiter (1995) in the energy range 0.05 eV < E_{cm} < 10^2 eV (classical calculation) and the cross section recommended by Phelps (1990) in the energy range 0.067 eV < E_{cm} < 6.67 keV (obtained interpolating results

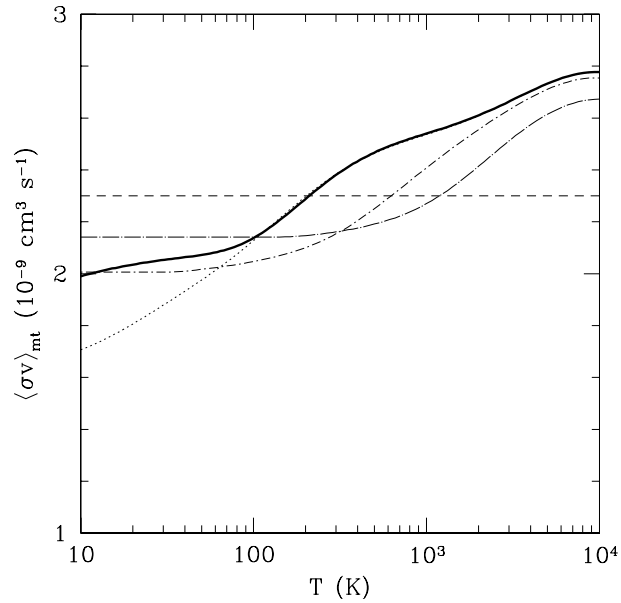

Fig. 5. The momentum transfer rate coefficient for H_3^+–H_2 collisions as function of the temperature T computed with the cross section shown in Fig. 4 for $v_d = 0$ (*thick solid* curve); $v_d = 1$ km s^{-1} (*dotted* curve); $v_d = 5$ km s^{-1} (*short-dash dotted* curve); and $v_d = 10$ km s^{-1} (*long-dash dotted* curve). The *dashed* line shows the Langevin rate.

from ion mobility experiments for E_{cm} < 2.3 eV and theoretical cross sections above 330 eV). As shown in Fig. 6, the quantal results depart significantly from the Langevin value at high energies (E_{cm} > 4 eV), and differ substancially from the results extrapolated from ion mobility experiments in the same energy range. Here we adopt the cross section computed by Krstić & Schultz (1999a,c), extrapolated to energies below 0.1 eV with the asymptotic formula $\sigma_{mt} = 1.05 \times 10^{-15}(E_{cm}/\text{eV})^{-0.531}$. We show in Fig. 7 the corresponding rate coefficient as a function of the temperature and the drift velocity. Again, the rate coefficient depends very weakly on these two quantities for temperatures below ~10^4 K.

3.4. e – H_2

The elastic scattering of electrons by H_2 has been the subject of much theoretical and experimental work of the past decades. In general, it is well established that the momentum transfer cross section for electron-molecule scattering deviates significantly from the classical Langevin rate at low energies (below ~1 eV), owing to the effect of "electron exchange", i.e., the exchange of the incoming electron with one orbital electron in the neutral species (see e.g., Massey & Ridley 1956; Morrison & Lane 1975). The existence of this effect has been confirmed experimentally by Ferch et al. (1980) in the energy range 0.02–2 eV. The net result is a reduction of the momentum transfer cross section, which compensates the polarization (Langevin) contribution in such a way that the resulting cross section is roughly constant at low-collision energies.

We have assembled a compilation of the available measurements of the e–H_2 momentum transfer cross section, for collision energies ranging from 10^{-3} eV up to 200 eV. A detailed summary of the most recent experimental results is given by Brunger & Buckman (2002). The results are shown in Fig. 8, compared with the theoretical calculations of Henry & Lane (1969) and the Langevin value. Clearly, the semi-classical

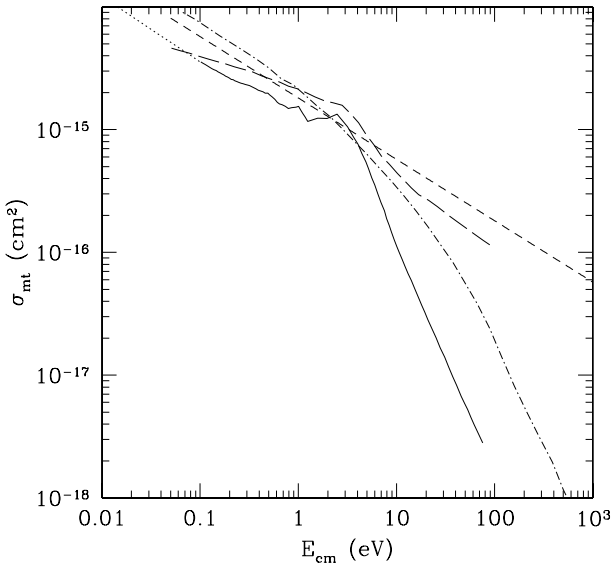

Fig. 6. The momentum transfer cross section for H^+–H_2 collisions as a function of E_{cm}: fully-quantal calculation by Krstić & Schultz (1999a,c) (*solid* curve), with our extrapolation to low energies (*dotted* line); classical calculation by Bachmann & Reiter (1995) (*long-dashed* curve); semi-empirical recommendations by Phelps (1990) (*dot-dashed* curve); Langevin cross section (*dashed* curve).

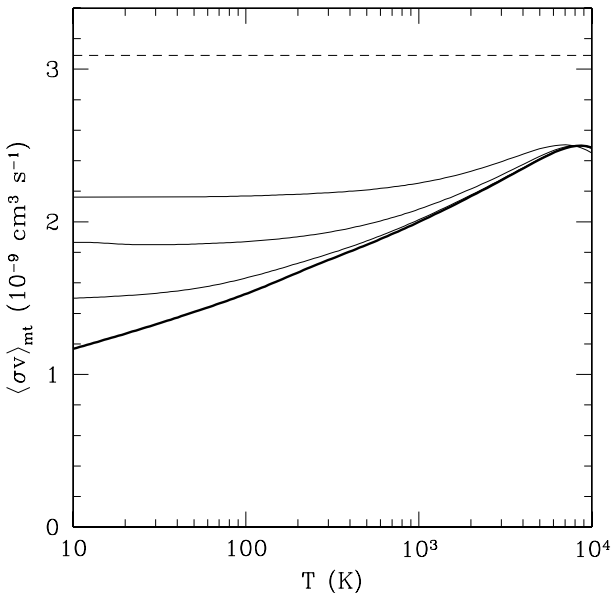

Fig. 7. The collision rate coefficient for H^+–H_2 collisions as a function of the temperature, computed with the momentum transfer cross section of Krstić & Schultz (1999a,c) for $v_d = 0$ (*thick solid* curve); and $v_d = 2$ km s^{-1}; $v_d = 4$ km s^{-1}; $v_d = 10$ km s^{-1} (*thin solid* curves, *bottom to top*). The *dashed* line shows the Langevin rate.

Langevin formula provides a poor approximation to the actual cross section, especially at energies below ∼1 eV, where the effects of "electron exchange" are dominant. The agreement between laboratory measurements and theoretical values of the scattering cross sections appear to be satisfactory, with the possible exception of the region of very low electron energies, where the possible existence of a Ramsauer-Townsend minimum in the momentum transfer cross section is not completely excluded (Ramanan & Freeman 1991). The momentum transfer collision rate calculated with the cross section indicated by the solid line in Fig. 8 is shown in Fig. 9. At temperatures typical of

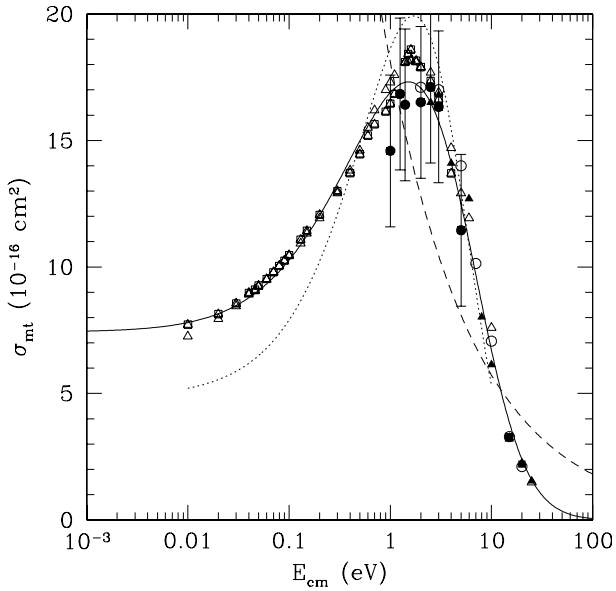

Fig. 8. The momentum transfer cross section for e–H_2 collisions as a function of the electron kinetic energy. Experimental values: England et al. (1988) (*empty triangles*), Schmidt et al. (1994) (*empty squares*), Shyn & Sharp (1981) (*empty circles*), Nishimura et al. (1985) (*filled triangles*), Khakoo & Trajmar (1986) (*filled squares*), Brunger et al. (1990, 1991) (*filled circles*). The *dashed* and *dotted* curves show the Langevin cross section and the quantum-mechanical theoretical results of Henry & Lane (1969), respectively. The *solid* curve shows the cross section adopted in this work.

interstellar clouds, $T \approx 10$ K, the Langevin formula overestimates the actual value of the momentum transfer rate by about two orders of magnitude.

4. Collisions with H

4.1. $C^+ - H$

The momentum transfer cross section for collisions of C^+ ions with H atoms was computed by Flower & Pineau-des-Forêts (1995) at several values of the collision energy, ranging from $E_{cm} \approx 5 \times 10^{-5}$ eV to $E_{cm} \approx 5$ eV with the adiabatic potential of Green et al. (1972) (see Fig. 10). Figure 11 shows the corresponding rate coefficient computed by integrating numerically our interpolation of the results of Flower & Pineau-des-Forêts (1995).

4.2. $H^+ - H$

Being the simplest ion-neutral collision process, the scattering of H^+ by H atoms has been the subject of a large number of theoretical investigations, from the semiclassical calculations of Dalgarno & Yadav (1953) to the accurate quantum mechanical calculations of Krstić & Schultz (1999a,c) and Glassgold et al. (2005, hereafter GKS). The latter paper, reporting a determination of the momentum transfer cross section over a range from 10^{-10} eV to 10^2 eV (partially shown in Fig. 12), represents the definitive reference on this elastic process. The only experimental determination of the H–H^+ momentum transfer cross section was obtained by Brennan & Morrow (1971) at $E_{cm} \approx 5$ eV by observing the velocity and attenuation of compressional Alfven waves propagating in a partially-ionized hydrogen plasma. The measured value, $\sigma_{mt} = 6.0^{+2.0}_{-1.5} \times 10^{-15}$ cm^2, is in good agreement with the quantum mechanical results (see

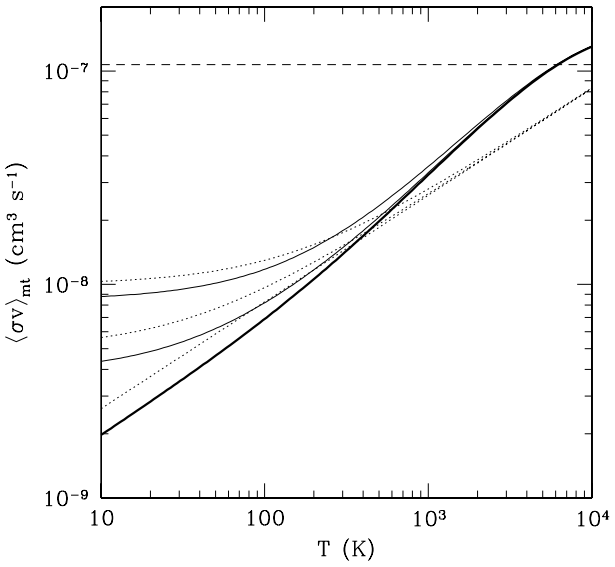

Fig. 9. The momentum transfer rate coefficient for e–H_2 collisions computed with the cross section shown in Fig. 8 as a function of the temperature T for $v_d = 0$ (*thick solid* curve); and $v_d = 50$ km s^{-1}; $v_d = 100$ km s^{-1} (*thin solid* curves, *top to bottom*), compared with the values computed with Eq. (14) of Draine (1983) for the same values of the drift velocity (*dotted* curve). The *dashed* line shows the Langevin rate.

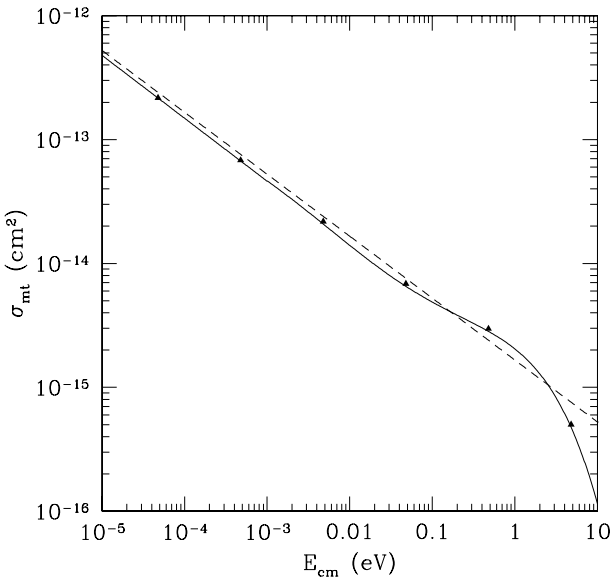

Fig. 10. The momentum transfer cross section for collisions C^+–H computed by Flower & Pineau-des-Fôrets (1995) as a function of the collision energy in the center-of-mass frame (original data, *triangles*; our interpolation, *solid* curve). The *dashed* curve shows the Langevin cross section.

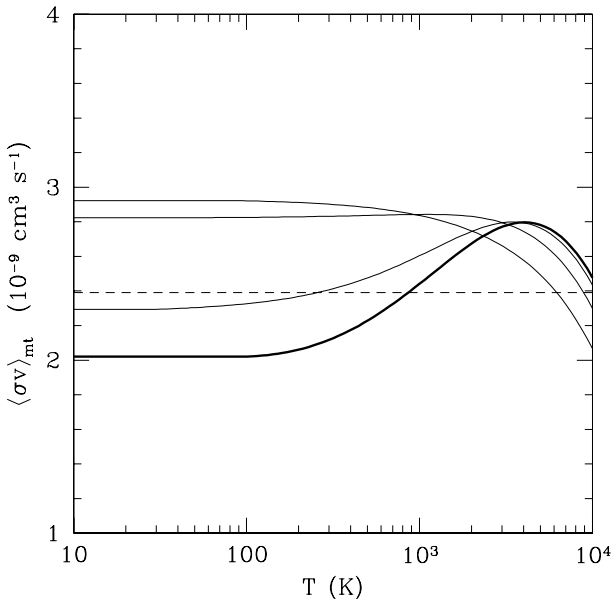

Fig. 11. The collision rate coefficient for collisions C^+–H as a function of the temperature for $v_d = 0$ (*thick solid* curve); and $v_d = 5$; $v_d = 10$; and $v_d = 15$ km s^{-1} (*thin solid* curves, *bottom to top*), compared with the Langevin rate (*dashed* line).

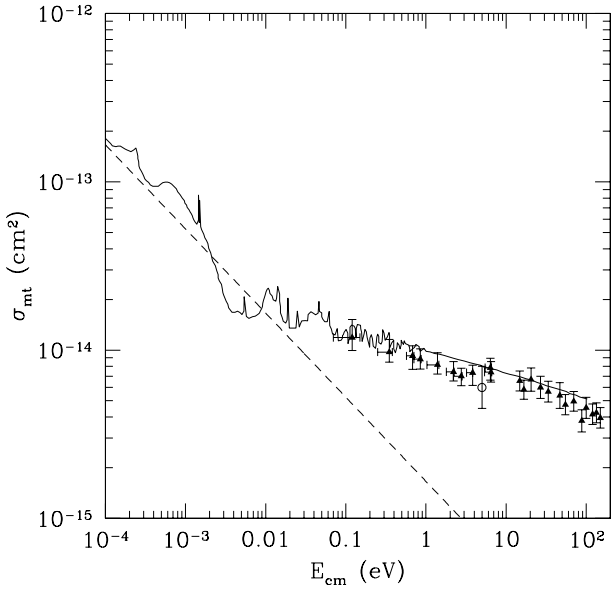

Fig. 12. The momentum transfer cross section for collisions H^+–H computed by GKS as a function of the collision energy in the center-of-mass frame (*solid* curve), compared to the Langevin cross section (*dashed* curve). The *empty circle* is the measurement by Brennan & Morrow (1971) at $E_{cm} \approx 5$ eV. The *filled triangles* are the values of the charge exchange cross section for the same interacting particles, measured by Newman et al. (1982), multiplied by 2.

Fig. 12). Previous estimates of the momentum transfer rate coefficient (Geiss & Bürgi 1986) were based on measurements and calculations of the charge exchange cross section σ_{ce} for the reaction $H + H^+ \rightarrow H^+ + H$ complemented at low energies with the polarization cross section computed with the Langevin formula Eq. (A.4). Since the charge transfer process proceeds with little momentum transfer between the interacting particles, Eq. (4) with $\Theta = \pi$ gives $\sigma_{mt} \approx 2\sigma_{ce}$ (Dalgarno 1958; Banks & Holzer 1968). As shown by Fig. 12, a combination of the polarization cross section and twice the value of the charge exchange cross section roughly reproduces the accurate results of GKS. However, the momentum transfer rate estimated by Geiss & Bürgi (1986) with this approximation for temperatures between 10^3 K and 2×10^4 K is about 50% higher than the rate obtained by a numerical integration of the momentum transfer cross section of GKS, shown in Fig. 13 for different values of the drift velocity.

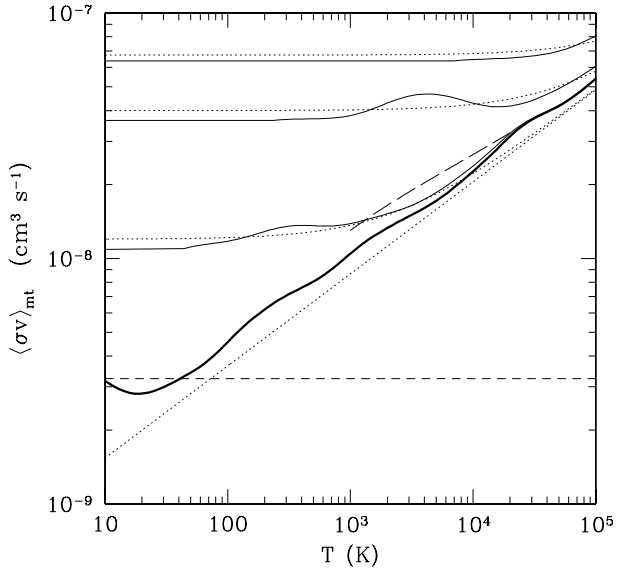

Fig. 13. The collision rate coefficient for collisions H^+–H as a function of the temperature for $v_{\rm d} = 0$ (*thick, solid* curve); $v_{\rm d} = 10$; $v_{\rm d} = 50$ km s^{-1}; and $v_{\rm d} = 100$ km s^{-1} (*thin, solid* curves, *bottom to top*); compared with the fitting formula of GKS for the same values of the drift velocity (*dotted* curves), the fitting formula of Geiss & Bürgi (1986) for $v_{\rm d} = 0$ (*long-dashed* curve) and the Langevin value (*short-dashed* curves).

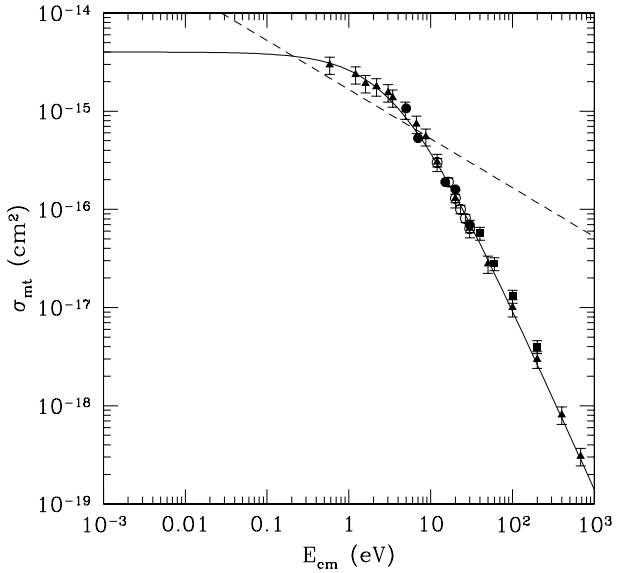

Fig. 14. Momentum transfer cross section for e–H collisions. Experimental values: Shyn & Cho (1989) (*filled circles*); Williams (1975a,b) (*filled triangles*); Shyn & Grafe (1992) (*filled squares*); Callaway & Williams (1975) (*empty circles*). The *solid* curve is the theoretical calculation of Dalgarno et al. (1999).

4.3. e – H

The momentum transfer cross section for e–H collisions has been computed by Dalgarno, et al. (1999) with the quantal formula of Dalgarno & Griffing (1958) and the phase shifts of Rudge (1975) and Das & Rudge (1976) at $E \lesssim 10$ eV, and by van Wyngaarden & Walters (1986) in the energy range 100–300 eV. Laboratory measurements of the e–H momentum transfer cross sections have been performed by Williams (1975a,b); Callaway & Williams (1975); Shyn & Cho (1989); Shyn & Grafe (1992) (for a detailed review of the experimental methods and results, see Bederson & Kieffer 1971; Trajmar & Kanik 1995). Theoretical and experimental results are shown in Fig. 14. The dependence of the cross section on collision energy is clearly non-Langevin: at low energies the cross section is approximately constant, $\sigma \approx 4 \times 10^{-15}$ cm^{-2}, whereas at high energies, it decreases with energy as $E_{\rm cm}^{-1.8}$. As a result, the momentum transfer rate, shown in Fig. 15, is lower by about one order of magnitude than the Langevin value at $T \approx 10$ K, and larger by ∼40% at $T \approx 10^4$ K, with a weak dependence on the relative drift velocity.

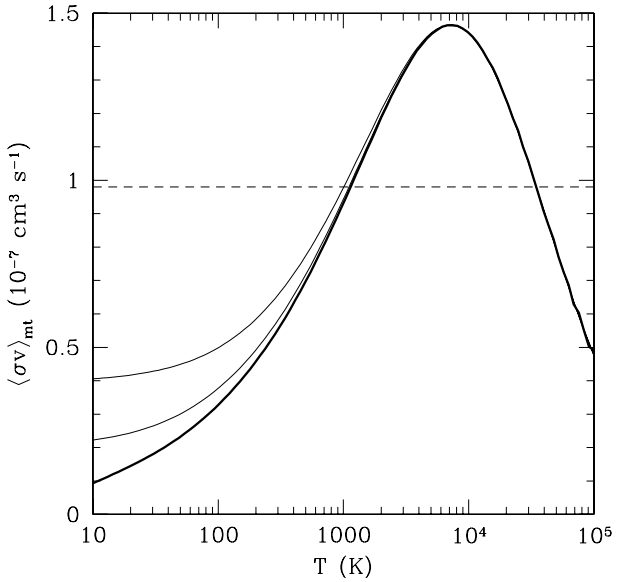

Fig. 15. Collision rate coefficient for e–H collisions as a function of temperature, for $v_{\rm d} = 0$ km s^{-1} (*thick* curve); $v_{\rm d} = 50$ km s^{-1}; and $v_{\rm d} = 100$ km s^{-1} (*thin* curves, *bottom to top*). The *dashed* line shows the Langevin rate.

5. Collisions with He

With the exception of collisions with H^+ or electrons, to our knowledge, there are no experimental or theoretical data available for elastic collisions between He atoms and charged species. An estimate based on the Langevin approximation (see Appendix), gives

$$\langle\sigma v\rangle_{i,\rm He} = \left[\frac{(m_i + m_{\rm He})m_n p_{\rm He}}{(m_i + m_n)m_{\rm He} p_n}\right]^{1/2} \langle\sigma v\rangle_{in}, \qquad (20)$$

where n = H or H_2, and p_n is the polarizability of species n (see Appendix). According to this equation, the momentum transfer rate for collision of ions with He is, in general, a factor 0.4–0.5 of the corresponding rate for collisions with H_2 and a factor 0.3–0.4 of the corresponding rate for collisions with H.

Collisions with He introduce a small correction to the expression of the friction coefficient α_{in} defined by Eq. (7). For a neutral component made of H_2 and He, Eq. (20) gives

$$\alpha_{in} \equiv \alpha_{i,\rm H_2} + \alpha_{i,\rm He} = c_i \alpha_{i,\rm H_2}, \qquad (21)$$

with

$$c_i = 1 + \left[\frac{(m_i + m_{\rm H_2})m_{\rm He} p_{\rm He}}{(m_i + m_{\rm He})m_{\rm H_2} p_{\rm H_2}}\right]^{1/2} \left(\frac{n_{\rm He}}{n_{\rm H_2}}\right). \qquad (22)$$

For example, for a cosmic He abundance of 0.1, the He correction factors based on the Langevin approximation are

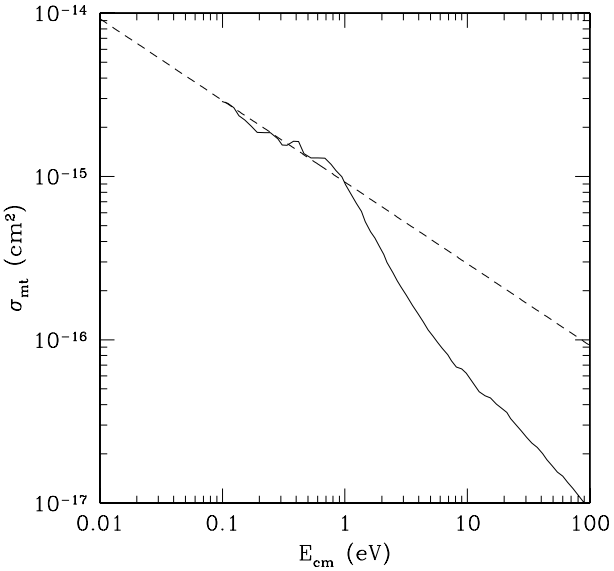

Fig. 16. The momentum transfer cross section for collisions H^+–He, according to the fully-quantal calculations of Krstić & Schultz (1999a,b), as a function of the collision energy in the center-of-mass frame (*solid* curve), compared to the Langevin cross section (*dashed* line).

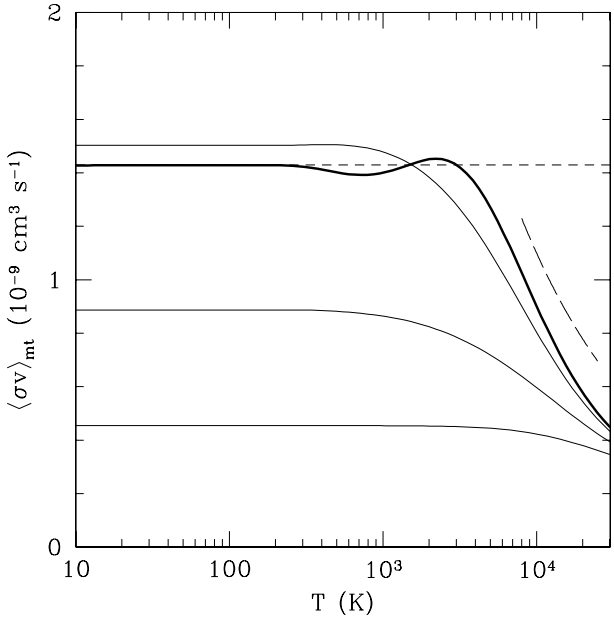

Fig. 17. The collisional rate coefficient for H^+–He collisions as a function of the temperature for $v_d = 0$ (*thick, solid* curve); $v_d = 10$ km s^{-1}; $v_d = 20$ km s^{-1}; and $v_d = 30$ km s^{-1} (*thin, solid* curves, *top to bottom*) compared with the fitting formula of Geiss & Bürgi (1986) for $v_d = 0$ (*long-dashed* curve) and the Langevin value (*short-dashed* curves).

$c_{H^+} = 1.12$, $c_{H_3^+} = 1.13$, and $c_{HCO^+} = 1.15$ (see also Mouschovias 1996). Similarly, for collisions with atomic hydrogen, the He correction for the H–H^+ rate coefficient is $c_{H^+} = 1.08$.

5.1. H^+ – He

Figure 16 shows the momentum transfer cross section for H^+–He collisions computed by Krstić & Schultz (1999a,b) with a semiclassical treatment in the energy range 0.1 eV < E_{cm} < 100 eV. The calculation has been recently extended up to 10^4 eV by Krstić & Schultz (2006). The theoretical results are in good agreement with the Langevin value below $E_{cm} \approx 1$ eV, but at larger energies the Langevin formula overestimates the theoretical results (by one order of magnitude at $E_{cm} \approx 100$ eV). To our knowledge, no experimental results are available for H^+–He collisions. Here we adopt the cross section computed by Krstić & Schultz (1999a,b), extrapolated to energies below 0.1 eV with the Langevin value. The resulting collisional rate coefficient is shown in Fig. 17 as a function of the temperature and the drift velocity. As for H^+–H_2 collisions, the rate coefficient depends very weakly on these two quantities for temperatures below ~10^3 K and drift speeds below ~10 km s^{-1}. The rate coefficient $\langle\sigma v\rangle_{H^+,He}$ is about 0.9 $\langle\sigma v\rangle_{H^+,H_2}$, whereas Eq. (20) gives a factor ~0.5.

5.2. e – He

Accurate values of the momentum transfer cross sections for e–He collisions have been obtained from mobility experiments (Crompton et al. 1967, 1970; Milloy & Crompton 1977; Ramanan & Freeman 1990). The agreement between different experimental evaluations is excellent, at the level of 1–2%. As in the case of e–H_2 collisions discussed in Sect. 3, the actual cross section deviates significantly from the classical Langevin value, owing to the quantum exchange of the incoming electron with one orbital electron of He. This is especially evident at low-collision energies, where the momentum transfer cross section is approximately constant. The rate coefficient $\langle\sigma v\rangle_{e,He}$ is a factor ~0.6 of $\langle\sigma v\rangle_{e,H_2}$.

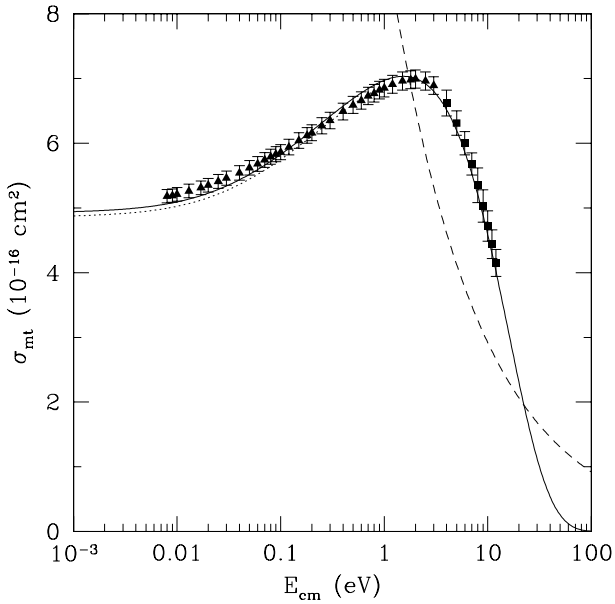

Fig. 18. The momentum transfer cross section for e–He collisions as a function of the electron kinetic energy. Experimental values: Crompton et al. (1970) (*filled triangles*); Milloy & Crompton (1977) (*filled squares*). The *dotted* curve shows the experimental results of Ramanan & Freeman (1990), with uncertainty ~3%. The *dashed* curve shows the Langevin cross section, whereas the *solid* curve is the cross section adopted in this work.

6. Collisions between dust grains and neutral particles

For collisions between a spherical grain g of charge $Z_g e$ and radius r_g with a neutral particle n of polarizability α_n, the

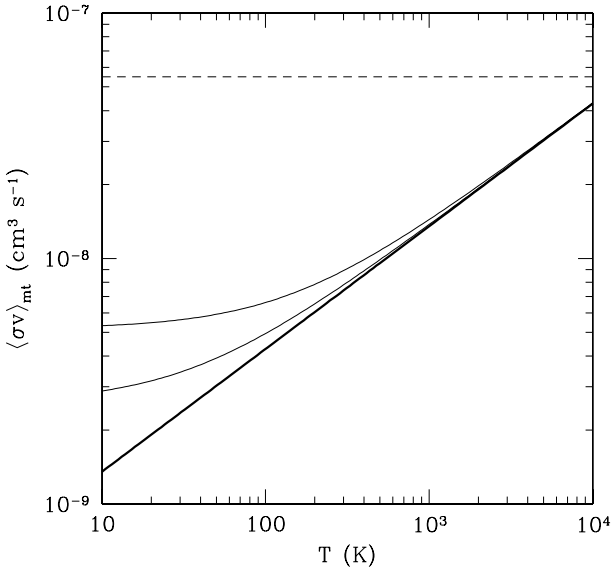

Fig. 19. The momentum transfer rate coefficient for e–He collisions computed with the cross section shown in Fig. 18 as a function of the temperature T for $v_d = 0$ (*thick, solid* curve); and $v_d = 50$ km s^{-1}; $v_d = 100$ km s^{-1} (*thin, solid* curves, *bottom to top*). The *dashed* line shows the Langevin rate.

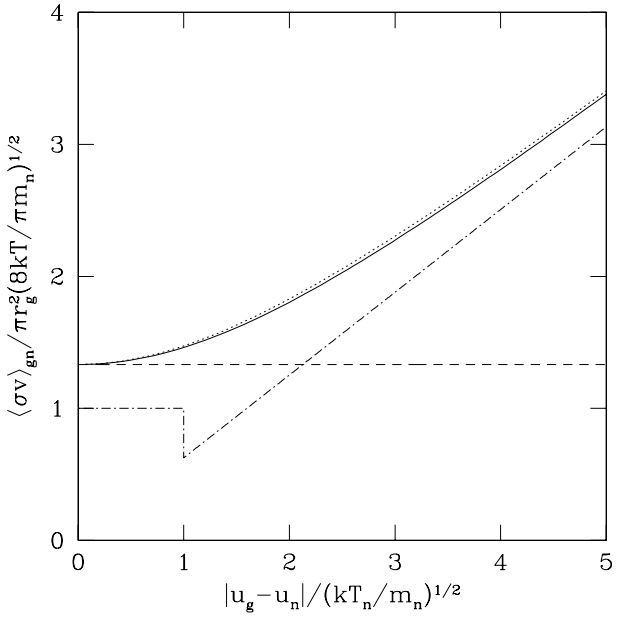

Fig. 20. Momentum transfer rate coefficient for collisions grain–neutral as a function of the relative drift velocity, from Eq. (15) with $n = 0$ (*solid* curve), compared with the expressions from Draine & Salpeter (1979) (*dotted* curve); Nakano (1984) (*dashed* curve); and Mouschovias & Ciolek (*dot-dashed* curve).

geometrical cross section πr_g^2 is larger that the polarization cross section (Eq. (A.4)) when

$$r_g > 24|Z_g|^{1/4}\left(\frac{\alpha_n}{\text{Å}^3}\right)^{1/4}\left(\frac{T_{ss'}}{\text{K}}\right)^{-1/4}\ \text{Å}, \tag{23}$$

a condition generally satisfied by interstellar grains. The average momentum transfer cross section for collisions of spherical grains with neutral atoms or molecules is then

$$\langle\sigma v\rangle_{gn} = \pi r_g^2\delta\left(\frac{2kT_{gn}}{\mu_{gn}}\right)^{1/2} G_0(\xi), \tag{24}$$

where $G_0(\xi)$ is given by Eq. (16) and δ is a factor of order unity (the so-called Epstein coefficient) equal to unity if the neutrals impinging on the grain undergo specular reflections. For very subsonic drift velocity, this expression reduces to

$$\langle\sigma v\rangle_{gn} \approx \frac{4}{3}\pi r_g^2\delta\left(\frac{8kT_n}{\pi m_n}\right)^{1/2}, \tag{25}$$

a result derived by Epstein (1924). Experiments with micron-size melamine-formaldehyde spheres show that $\delta \approx 1.3$ (Liu et al. 2003).

Figure 20 shows the grain-neutral momentum transfer rate as a function of the relative drift velocity according to Eq. (24) with $\delta = 1$ compared with the approximations given by Draine & Salpeter (1979), Nakano (1984), and Mouschovias & Ciolek (1999). In this figure, the grain-neutral momentum transfer rate is normalized to the expression given by Mouschovias & Ciolek (1999) in the low-drift limit, and the drift velocity is normalized to the mean thermal speed in the neutrals.

7. Collisions between charged particles

Particles of charge $Z_{s'}e$ can exchange momentum with particles of charge Z_se and density n_s via long-range Coulomb interactions. In the standard Coulomb scattering theory (see e.g., Chapman & Cowling 1953), the momentum transfer cross section is given by

$$\sigma_{mt} = 2\pi r_C^2(v_{ss'})\ln\left[\frac{r_C^2(v_{ss'}) + r_{max}^2}{r_C^2(v_{gs}) + r_{min}^2}\right], \tag{26}$$

where

$$r_C(v_{ss'}) = \frac{Z_sZ_{s'}e^2}{\mu_{ss'}v_{ss'}^2} \tag{27}$$

is the Coulomb radius (the distance at which the electrostatic energy is of the order of the kinetic energy) at the relative velocity $v_{ss'}$, and r_{min}, r_{max} are the minimum and maximum impact parameters of the collision. Several different approaches have been taken to calculate r_{min} and r_{max}. For the latter, the standard choice is the total Debye length in the plasma λ_D (Cohen et al. 1950), given by

$$\frac{1}{\lambda_D^2} = \sum_s\frac{1}{\lambda_{D,s}^2} = \frac{4\pi e^2}{k}\sum_s\frac{Z_s^2n_s}{T_s}. \tag{28}$$

When averaging over the relative velocity of interacting particles (Eq. 8), the slowly varying logarithmic factor can be considered constant, and the term $r_C(v_{ss'})$ in the logarithm's argument can be replaced by

$$\overline{r_C} \equiv r_C(\langle v_{ss'}^2\rangle) = \frac{Z_sZ_{s'}e^2}{3kT_{ss'}}, \tag{29}$$

where $\langle v_{ss'}^2\rangle = 3kT_{ss'}/\mu_{ss'}$ is the average of the square of the relative velocity (Spitzer 1956). The averaging of the remaining dependence of the cross section on the inverse fourth power of the relative velocity then gives, according to Eq. (15),

$$\langle\sigma v\rangle_{ss'} = 2\pi a_{ss'}r_C^2(a_{ss'})\ln\left[\frac{\overline{r_C}^2 + \lambda_D^2}{\overline{r_C}^2 + r_{min}^2}\right]G_4(\xi), \tag{30}$$

where $a_{ss'}$ is given by Eq. (11) and $G_4(\xi)$ by Eq. (17). If the particles are assumed to be pointlike ($r_{\rm min} = 0$), and, in addition, $\lambda_{\rm D} \gg \overline{r_{\rm C}}$ (a condition generally fulfilled in the ISM), we have

$$\ln\left[1 + \left(\frac{\lambda_{\rm D}}{\overline{r_{\rm C}}}\right)^2\right] \approx 2\ln\left(\frac{\lambda_{\rm D}}{\overline{r_{\rm C}}}\right). \quad (31)$$

In this case Eq. (30) for $\xi = 0$ gives the standard expression of the Coulomb momentum transfer rate (Spitzer 1956)

$$\langle\sigma v\rangle_{ss'} = \frac{16\pi^{1/2} Z_s^2 Z_{s'}^2 e^4}{3\mu_{ss'}^{1/2}(2kT_{ss'})^{3/2}} \ln\Lambda_{ss'}$$
$$\approx 8.48\times10^{-2} Z_s^2 Z_{s'}^2 \left(\frac{\mu_{ss'}}{m_{\rm H}}\right)^{-1/2}\left(\frac{T}{K}\right)^{-3/2}\ln\Lambda, \quad (32)$$

where

$$\ln\Lambda_{ss'} \equiv \ln\left(\frac{\lambda_{\rm D}}{\overline{r_{\rm C}}}\right) = \ln\left[\frac{3kT_{ss'}}{Z_s Z_{s'} e^2}\left(\frac{4\pi e^2}{k}\sum_s \frac{Z_s^2 n_s}{T_s}\right)^{-1/2}\right] \quad (33)$$
$$= 9.42 - \ln\left\{\frac{Z_s Z_{s'}}{(T_{ss'}/{\rm K})}\left[\sum_s \frac{Z_s^2 (n_s/{\rm cm}^{-3})}{(T_s/{\rm K})}\right]^{1/2}\right\}, \quad (34)$$

is the *Coulomb logarithm*.

7.1. Collisions of ions with charged dust grains

In astrophysical applications, Eq. (32) has often been adopted to compute the rate of momentum transfer between grain-ion and grain-electron collisions (Draine & Salpeter 1979). However, a more accurate calculation requires a modification of the Coulomb logarithm to account for the finite size of the grains. Taking $r_{\rm min} = r_{\rm g}$ in Eq. (30), and assuming as before $\lambda_{\rm D} \gg \overline{r_{\rm C}}$, we obtain the modified Coulomb logarithm for grain-ion (or grain-electron) collisions

$$\ln\Lambda_{\rm gi} = \ln\left[\frac{\lambda_{\rm D}}{(\overline{r_{\rm C}}^2 + r_{\rm g}^2)^{1/2}}\right], \quad (35)$$

which reduces to $\ln(\lambda_{\rm D}/\overline{r_{\rm C}})$ for $r_{\rm g} = 0$, and approaches $\ln(\lambda_{\rm D}/r_{\rm g})$ for $r_{\rm g} \gg \overline{r_{\rm C}}$. The latter value of the Coulomb logarithm has been used, e.g., by Benkadda et al. (1996) in their study of nonlinear instabilities in dusty plasmas. Following Draine & Sutin (1987), it is easy to compute the ratio $r_{\rm g}/\overline{r_{\rm C}}$ for a variety of astrophysical conditions, since this quantity depends almost exclusively on the reduced temperature $\tau_i \equiv r_{\rm g} kT_i/(Z_i e)^2$,

$$\frac{r_{\rm g}}{\overline{r_{\rm C}}} = \frac{3Z_i\tau_i}{Z_{\rm g}(\tau_i)}. \quad (36)$$

Using the analytical approximations for the value of the average grain charge $Z_{\rm g}e$ as a function of τ_i computed by Draine & Sutin (1987), we obtain the modified Coulomb logarithm for grain-ion collisions given in Fig. 21 for "light" and "heavy ions" (effective atomic weight 1 and 25, respectively). We see from this figure that the pointlike approximation for the Coulomb logarithm remains valid for τ_i less than ~0.1. For larger values of τ_i the value of the Coulomb logarithm is smaller than the pointlike value, but the effect is a reduction of the constant in Eq. (34), from 9.42 to 8.97 or 9.18 at worst, for the "light ion" and "heavy ion" cases, respectively.

For a more general calculation of the Coulomb logarithm for grain-ion and grain-electron where $r_{\rm min}$ depends on the finite size of the grain and the relative velocity of the collision, and, in addition, the approximation $\lambda_{\rm D} \gg \overline{r_{\rm C}}$ is removed, see Khrapak & Morfill (2004).

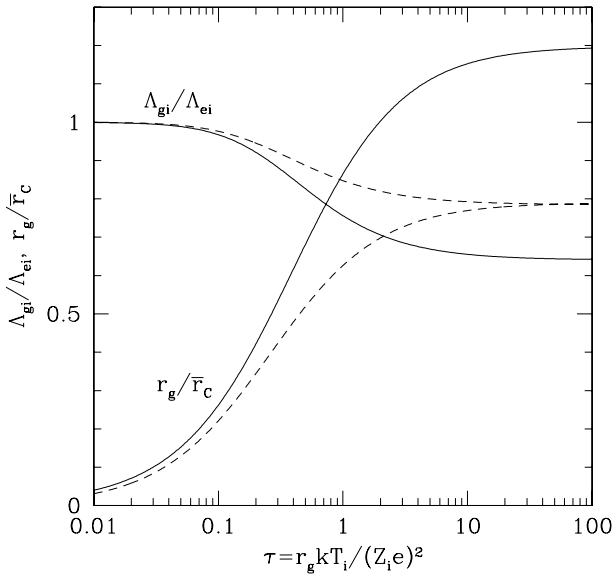

Fig. 21. Argument of the Coulomb logarithm $\Lambda_{\rm gi}$ for grain-ions interactions normalized to Λ_{ei} for pointlike particles, and ratio $r_{\rm g}/\overline{r}_{\rm C}$ as a function of the reduced temperature of the ions $\tau_i = r_{\rm g}kT_i/(Z_i e)^2$. The *solid* and *dashed curves* are for "light ions" with effective atomic weight 1 and "heavy ions" with effective atomic weight 25.

Table 1. Fitting formulae for momentum transfer coefficients as a function of the gas temperature T (in K) and $\theta \equiv \log(T/{\rm K})$ for $v_{\rm d} = 0$.

Species s, s'	$\langle\sigma v\rangle_{ss'}$ (10^{-9} cm^3 s^{-1})
HCO^+, H_2	$T^{1/2}(1.476 - 1.409\theta + 0.555\theta^2 - 0.0775\theta^3)$
H_3^+, H_2	$2.693 - 1.238\theta + 0.664\theta^2 - 0.089\theta^3$
H^+, H_2	$1.003 + 0.050\theta + 0.136\theta^2 - 0.014\theta^3$
e, H_2	$T^{1/2}(0.535 + 0.203\theta - 0.163\theta^2 + 0.050\theta^3)$
C^+, H	$1.983 + 0.425\theta - 0.431\theta^2 + 0.114\theta^3$
H^+, H	$0.649T^{0.375}$ (GKS)
e, H	$T^{1/2}(2.841 + 0.093\theta + 0.245\theta^2 - 0.089\theta^3)$
H^+, He	$1.424 + 7.438\times10^{-6}T - 6.734\times10^{-9}T^2$
e, He	$0.428T^{1/2}$

8. Analytical approximations

In Table 1 we list analytical fitting formulae for the momentum transfer rate coefficients computed numerically in Sects. 3–5. For zero drift velocity, we have approximated the rates (or their logarithm) with third-order polynomials of the logarithm of the temperature. The accuracy of these fitting formulae is ~10%. The dependence on the drift velocity has been approximated, following GKS and Draine (1980) by power-laws (or modified power-laws) fits of the numerical results in terms of the rms velocity, defined as

$$v_{\rm rms} \equiv \left(v_{\rm d}^2 + \frac{8kT_{ss'}}{\pi\mu_{ss'}}\right)^{1/2}. \quad (37)$$

These fitting formulae are shown in Table 2. Within the range of $v_{\rm rms}$ indicated, the accuracy of the power-law approximations is better than ~20%.

9. Conclusions

We have derived momentum transfer coefficients for collisions between ions, electrons, charged dust grains and

Table 2. Fitting formulae for momentum transfer coefficients as function of $v_{\rm rms}$ (in km s^{-1}).

Species s, s'	$\langle\sigma v\rangle_{ss'}$ (cm^3 s^{-1})	$v_{\rm rms}$ (km s^{-1})
HCO^+, H_2	$2.40\times10^{-9}v_{\rm rms}^{0.6}$	$0.2\lesssim v_{\rm rms}\lesssim 5$
H_3^+, H_2	$2.00\times10^{-9}v_{\rm rms}^{0.15}$	$1\lesssim v_{\rm rms}\lesssim 10$
H^+, H_2	$3.89\times10^{-9}v_{\rm rms}^{-0.02}$	$1\lesssim v_{\rm rms}\lesssim 10$
e, H_2	$3.16\times10^{-11}v_{\rm rms}^{1.3}$	$20\lesssim v_{\rm rms}\lesssim 200$
C^+,H	$1.74\times10^{-9}v_{\rm rms}^{0.2}$	$2\lesssim v_{\rm rms}\lesssim 20$
H^+,H	$2.13\times10^{-9}v_{\rm rms}^{0.75}$	$v_{\rm rms}\gtrsim 1$ (GKS)
e, H	$2.50\times10^{-10}v_{\rm rms}^{1.2}\exp(-v_{\rm rms}/460)$	$20\lesssim v_{\rm rms}\lesssim 600$
H^+, He	$1.48\times10^{-9}v_{\rm rms}^{-0.02}$	$0.1\lesssim v_{\rm rms}\lesssim 10$
e, He	$7.08\times10^{-11}v_{\rm rms}$	$20\lesssim v_{\rm rms}\lesssim 500$

atomic/molecular hydrogen from available experimental data and theoretical calculations, within the classic approach developed by Boltzmann (1896) & Langevin (1905). The numerical results have been approximated with simple analytical functions of the temperature and the drift velocity between the colliding species. The main conclusions of our study are the following:

1. For collisions between molecular ions (HCO^+, H_3^+) and H_2, the often used polarization approximation valid for an induced electric dipole attraction is in satisfactory agreement (within 20–50% of the numerical results). At low temperatures (10–50 K) and for low values of the drift velocities, the polarization approximation overestimates the actual rate for collisions between H^+ and H_2 by a factor of ∼3. In heavily-depleted molecular cloud cores, where H^+ may be the dominant ion (see, e.g., Walmsley et al. 2004), the Langevin approximation should not be used to compute ambipolar diffusion time scales (see Paper I).
2. For collisions between electrons and H_2, which contribute marginally to the resistivity of the interstellar gas (see Paper I), the polarization approximation fails by orders of magnitude because of the non-dipolar nature of the interaction, especially at low energies.
3. In the range 10 K $\lesssim T \lesssim 10^3$ K, rate coefficients for collisions between H^+ and He atoms are a factor 0.7–1 and 0.1–0.4 of the corresponding rate for collisions with H_2 and H, respectively. In the same temperature range, the rate coefficient for e–He collisions is a factor 0.4–0.7 of the rate for e–H_2 collisions and a factor 0.1–0.3 of the rate for e–H collisions.
4. Grain-neutral and grain-ion collisions are well represented by hard-spheres and Coulomb interactions, respectively. In the latter case, slightly different expressions may be adopted for the Coulomb logarithm, with no significant consequences for applications to ISM grains.

Acknowledgements. We thank A. Glassgold for helpful discussions and for making available to us data on elastic cross sections. The research of D.G. is partially supported by the Marie Curie Research Training networks "Constellation".

Appendix: Polarization approximation

The cross section for the interaction between an ion i of charge Z_ie and a neutral molecule (or atom) n is determined by the attractive polarization potential

$$V_{in}(r) = -\frac{p_n Z_s e^2}{2r^4}, \tag{A.1}$$

where r is the distance between the centers of the ion and the molecule (much larger than the sizes of the ion and molecule) and α_n is the polarizability of the molecule. The relative cross section can be calculated from the classical trajectories allowed by this potential (see, e.g., Dalgarno et al. 1958a,b; Mitchner & Kruger 1973), and is

$$\sigma(v_{in}) = 2.210\pi\left(\frac{p_n Z_i e^2}{\mu_{in} v_{in}^2}\right)^{1/2}. \tag{A.2}$$

In this polarization approximation, the rate coefficient ("Langevin rate") is given by

$$\langle\sigma v\rangle_{in} = 2.210\pi\left(\frac{p_n Z_s e^2}{\mu}\right)^{1/2}, \tag{A.3}$$

which is independent of the gas temperature and the relative drift of the interacting species. Osterbrock (1961) corrected the numerical coefficient 2.21 in 2.41 to account for the repulsive nature of the interaction potential at small r, assuming that for small impact parameters the scattering is on average isotropic.

The Langevin cross section for collisions of ions with neutrals, taking into account Osterbrok's (1961) correction, therefore, results in

$$\sigma_{\rm in}(E_{\rm cm}) = 2.03\times10^{-15}Z_i^{1/2}\left(\frac{p_n}{\text{Å}^3}\right)^{1/2}\left(\frac{E_{\rm cm}}{\rm eV}\right)^{-1/2}\ {\rm cm}^2, \tag{A.4}$$

and the corresponding rate is

$$\langle\sigma v\rangle_{in} = 2.81\times10^{-9}Z_i^{1/2}\left(\frac{p_n}{\text{Å}^3}\right)^{1/2}\left(\frac{\mu_{in}}{m_{\rm H}}\right)^{-1/2}\ {\rm cm}^3\ {\rm s}^{-1}. \tag{A.5}$$

Values of the polarizability are $p_{\rm H} = 0.667$ Å^3, $p_{\rm H_2} = 0.804$ Å^3, and $p_{\rm He} = 0.207$ (Osterbrock 1961).

References

Abramowitz, M., & Stegun, I. A. 1965, Handbook of Mathematical Functions (New York: Dover)
Bachmann, P., & Reiter, D. 1995, Control Plasma Phys., 35, 45
Baines, M. J., Williams, I. P., & Asebiomo, A. S. 1965, MNRAS, 130, 63
Banks, P. M., & Holzer, T. E. 1968, Planet. Space Sci., 16, 1019
Bederson, B., & Kieffer, L. J. 1971, Rev. Mod. Phys., 43, 601
Benkadda, S., Gabbai, P., Tsytovich, V. N., & Verga, A. 1996, Phys. Rev. E, 53, 2717
Boltzmann, L. 1896, Vorlesungen über Gastheorie (Leipzig: Barth), 1, 119
Brennan, M. H., & Morrow, R. 1971, J. Phys. B, 4, L53
Brunger, M. J., & Buckman, S. J. 2002, Phys. Rep., 357, 215
Brunger, M. J., Buckman, S. J., & Newman, D. S. 1990, Austr. J. Phys., 43, 665
Brunger, M. J., Buckman, S. J., Newman, D. S., & Alle, D. T. 1991, J. Phys. B, 24, 1435.
Callaway, J., & Williams, J. F. 1975, Phys. Rev. A., 12, 2312
Chapman, S., & Cowling, T. G. 1953, The Mathematical Theory of Non-Uniform Gases (Cambridge: University Press)
Chandrasekhar, S. 1943, ApJ, 97, 255
Cohen, R. S., Spitzer, L., & Routley, P. 1950, Phys. Rev., 80, 230
Crompton, R. W., Elford, M. T., & Jory, R. L. 1967, Aust. J. Phys., 20, 369
Crompton, R. W., Elford, M. T., & Robertson, A. G. 1970, Austr. J. Phys., 23, 667
Dalgarno, A. 1958, J. Atmos. Terr. Phys., 12, 219
Dalgarno, A., & Yadav, H. N. 1953, Proc. Phys. Soc. A, 66, 173
Dalgarno, A., & Griffing, G. W. 1958, Proc. R. Soc. London A, 248, 415
Dalgarno, A., McDowell, M. R. C., & Williams, A. 1958a, Phil. Trans. Roy. Soc. (London), A-250, 411
Dalgarno, A., McDowell, M. R. C., & Williams, A. 1958b, Phil. Trans. Roy. Soc. (London), A-250, 426
Dalgarno, A., Yan, M., & Liu, W. 1999, ApJ, 125, 237
Das, J. N., & Rudge, M. R. H. 1976, J. Phys. B, 10, 3741
Draine, B. T. 1980, ApJ, 241, 1021

Draine, B. T., & Salpeter, E. E. 1979, ApJ, 231, 77
Draine, B. T., & Sutin, B. 1987, ApJ, 320, 803
Draine, B. T., Roberge, W. G., & Dalgarno, A. 1983, ApJ, 264, 485
Dreicer, H. 1959, Phys. Rev., 115, 238
Ellis, H. W., Pai, R. Y., McDaniel, E. W., Mason, E. A., & Vieland, L. A. 1976, Atomic Data Nucl. Data Tables, 17, 177
England, J. P., Elford, M. T., & Crompton, R. W. 1988, Aust. J. Phys., 41, 573
Epstein, P. S. 1924, Phys. Rev., 23, 710
Ferch, J., Raith, W., & Schroder, K. 1980, J. Phys. B, 13, 1481
Flower, D. R. 2000, MNRAS, 313, L19 (erratum in MNRAS, 315, 431)
Flower, D. R., & Pineau des Forêts, G. 1995, MNRAS, 275, 1049
Geiss, J., & Bürgi, A. 1986, A&A, 159, 1
Glassgold, A. E., Krstić, P. S., & Schultz, D. R. 2005, ApJ, 621, 808 (GKS)
Green, S., Bagus, P. S., Liu, B., McLean A. D., & Yoshimine, M. 1972, Phys. Rev. A, 5, 1614
Henry, R. J. W., & Lane, N. F. 1969, Phys. Rev., 183, 221
Khakoo, M. A., & Trajmar, S. 1986, Phys. Rev. A, 34, 138
Khrapak, S. A., & Morfill, G. E. 2004, Phys. Rev. E, 69, 66411
Krstić, P. S., & Schultz, D. R. 1999a, Atomic Plasma-Material Interaction Data for Fusion, 8, 1 (APID Series)
Krstić, P. S., & Schultz, D. R. 1999b, J. Phys. B, 32, 2415
Krstić, P. S., & Schultz, D. R. 1999c, Phys. Rev., 60, 2118
Krstić, P. S., & Schultz, D. R. 2006, Phys. Plasmas, 13, 053501
Langevin, P. 1905, Annales de Chimie et de Physique, Series 8, 5, 245, english translation in Appendix II of McDaniel (1964), cit
Liu, B., Goree, J., Nosenko, V., & Boufendi, L. 2003, Phys. Plasmas, 10, 9
Massey, H. S. W., & Ridley, R. O. 1956, Proc. Phys. Soc. A, 69, 659
Maxwell, J. C. 1860a, Phil. Mag., 19, 19
Maxwell, J. C. 1860b, Phil. Mag., 20, 21
McDaniel, E. 1964, Collision Phenomena in Ionized Gases (New York: Wiley)
Mestel, L., & Spitzer, L. 1956, MNRAS, 116, 503
Milloy, H. B., & Crompton, R. W. 1977, Phys. Rev. A, 15, 1847
Mitchner, M., & Kruger, C. H., 1973, Partially Ionized Gases (New York, Wiley)
Morrison, M. A., & Lane, N. F. 1975, Phys. Rev. A, 12, 2361
Mouschovias, T. C. 1996, in Solar and Astrophysical Magnetohydrodynamical Flows, ed. K. Tsinganos (Dordrecht: Kluwer), 505
Mouschovias, T. C., & Ciolek, G. E. 1999, in The Origin of Stars and Planetary Systems, ed. C. J. Lada, & N. D. Kilafis (Dordrecht: Kluwer), 305
Nakano, T. 1984, Fund. Cosm. Phys., 9, 139
Newman, J. H., Cogan, J. D., Ziegler, D. L., et al. 1982, Phys. Rev. A, 25, 2976
Nishimura, H., Danjo, A., & Sugahara, H. 1985, J. Phys. Soc. Japan, 54, 1757
Osterbrock, D. 1961, ApJ, 134, 260
Phelps, A. V. 1990, J. Phys. Chem. Ref. Data, 19, 653
Pinto, C., Galli, D., & Bacciotti, F. 2008, A&A, 484, 1
Ramanan, G., & Freeman, G. R. 1990, J. Chem Phys., 93, 3120
Ramanan, G., & Freeman, G. R. 1991, J. Chem Phys., 95, 4195
Rudge, M. R. H. 1975, J. Phys. B, 8, 940
Scalo, J. M. 1977, ApJ, 213, 705
Schmidt, B., Berkhan, K., Götz, B., & Müller, M. 1994, Phys. Scr., T53, 30
Shyn, T. W., & Sharp, W. E. 1981, Phys. Rev. A, 24, 1734
Shyn, T. W., & Cho, S. Y. 1989, Phys. Rev. A, 40, 1315
Shyn, T. W., & Grafe, A. 1992, Phys. Rev. A, 46, 2949
Sivukhin, D. V. 1966, in Reviews of Plasma Physics, 4, 93 (russian orig. 1964)
Spitzer, L. 1956, Physics of Fully Ionized Gases (New York: Interscience), 78
Trajmar, S., & Kanik, I. 1995, in Atomic and Molecular Processes in Fusion Edge Plasmas, ed. R. K. Janev (New York: Plenum Press), 31
Walmsley, C. M., Flower, D. R., & Pineau des Forêts, G. 2004, A&A, 418, 1035
Williams, J. F. 1975a, J. Phys. B, 8, 1683
Williams, J. F. 1975b, J. Phys. B, 8, 2191
van Wyngaarden, W. L., & Walters, H. R. J. 1986, J. Phys. B, 19, L53
Zweibel, E. G., & Josafatsson, K. 1983, ApJ, 270, 511